

# We are IntechOpen, the world's leading publisher of Open Access books Built by scientists, for scientists

6,900

Open access books available

185,000

International authors and editors

200M

Downloads

Our authors are among the

154

Countries delivered to

TOP 1%

most cited scientists

12.2%

Contributors from top 500 universities



WEB OF SCIENCE™

Selection of our books indexed in the Book Citation Index  
in Web of Science™ Core Collection (BKCI)

Interested in publishing with us?  
Contact [book.department@intechopen.com](mailto:book.department@intechopen.com)

Numbers displayed above are based on latest data collected.  
For more information visit [www.intechopen.com](http://www.intechopen.com)



# OAM Modes in Optical Fibers for Next Generation Space Division Multiplexing (SDM) Systems

*Alaaeddine Rjeb, Habib Fathallah and Mohsen Machhout*

## Abstract

Due to the renewed demand on data bandwidth imposed by the upcoming capacity crunch, optical communication (research and industry) community has oriented their effort to space division multiplexing (SDM) and particularly to mode division multiplexing (MDM). This is based on separate/independent and orthogonal spatial modes of optical fiber as data carriers along optical fiber. Orbital Angular Momentum (OAM) is one of the variants of MDM that showed promising features including the efficient enhancement of capacity transmission from Tbit to Pbit and substantial improvement of spectral efficiency up to hundreds ( $\text{bs}^{-1} \text{Hz}^{-1}$ ). In this chapter, we review the potentials of harnessing SDM as a promising solution for next generation global communications systems. We focus on different SDM approaches and we address specifically the MDM (different modes in optical fiber). Finally, we highlight the recent main works and achievements that have been conducted (in last decade) in OAM-MDM over optical fibers. We focus on main R&D activities incorporating specialty fibers that have been proposed, designed and demonstrating in order to handle appropriate OAM modes.

**Keywords:** Space Division Multiplexing (SDM), Mode Division Multiplexing (MDM), Orbital Angular Momentum (OAM), Specialty optical fibers

## 1. Introduction

Bandwidth-hungry applications and services, such as HDTV, big data, quantum computing, 5G/6G communication, industry 4.0 and game streaming, in addition to the exponential increase of users and connected devices (Internet of Things: IOT), may cause a capacity crunch in near future [1–3]. While other physical limitations behind the capacity crunch are based on the nonlinear Shannon limit and the scalability of actually deployed devices. The cited emerging applications (i.e. paradigms) has pushed telecommunications community (researchers & industries) to grow through multiple stages by developing higher capacity optical networks in optical fiber based links targeting to deal with the evolution of the market need for telecoms and Internet data services and paving the road to surpass the upcoming capacity limit challenges [4].

Recently, the capacity and the spectral efficiency of optical fibers have been substantially improved (i.e. scaling by several orders of magnitude) by using different multiplexing techniques and advanced optical modulation formats.

These multiplexing techniques are based on the exploitation of degrees of freedom of the optical signal to encode data information. The time, as time division multiplexing (TDM: interleaving channels temporally), the polarization, Polarization division multiplexing (PDM), the wavelength, as wavelength division multiplexing (WDM: using multiple wavelength channels) and the phase (quadrature) are examples of such techniques [5].

Research and industrial community had recently oriented their effort towards Space Division Multiplexing (SDM) techniques that is based on the exploitation of the spatial structure of the light or the physical transmission medium to encode information. Simply, SDM consists of increasing the number of data channels available inside an optical fiber. Two attractive embodiments of SDM are core division multiplexing (CDM) and mode division multiplexing (MDM) [6]. CDM is simply considered as the increasing of parallel single mode cores, carrying information, embedded in the same cladding of optical fiber (known as multicore fiber MCF) or single core fibers bundles [7]. Mode division multiplexing (MDM) is based on excitation and propagation of several spatial optical modes as individual/separate/independent data channels within common physical transmission medium targeting to boost the capacity transmission [8]. MDM is realized by multimode fibers generally over short haul interconnect transmission or few mode fibers as transmission medium for long haul transmission link. Numerous mode basis have been used for mode division multiplexing showing its effectiveness to scale up from Terabit to Petabit the capacity transmission and unleash from dozen to hundred (bit/s/Hz) the spectral efficiency over optical fiber.

It is well known that light can carry Angular Momentum (AM) that expresses the amount of dynamical rotation present in the electromagnetic field representing the light. The AM of light beam is divided into two distinct forms of rotation: Spin Angular Momentum (SAM) and Orbital Angular Momentum (OAM) [9]. The SAM is related to the polarization of light (e.g. right or left in circular polarization) while the OAM is related to the spiral phase front of  $\exp(jl\varphi)$  where  $l$  is a topological charge number (arbitrary unlimited integer), and  $\varphi$  is the azimuthal angle. Orbital angular momentum (OAM) of light, (known as twisted light), an additional degree of freedom, is arguably one of the most promising approaches that has recently deserved a special attention in optical fiber networks. Benefiting from two inherent features, which are:

(1) The orthogonality: where as a definition two signals are orthogonal, if data sent in these two dimensions can be uniquely separated from one another at the receiver without affecting each other's detection performance. Two OAM modes with different charge number  $l$  do not interfere.

(2) The unlimiteness: the charge number  $l$  is theoretically infinite. Hence, Each OAM mode (each specifically  $l$ ) is an independent data channels. OAM modes has been harnessed in multiplexing/de-multiplexing (OAM-MDM) or in increasing the overall optical channel capacity [10, 11].

As any promising technology, OAM-MDM through optical fibers is facing several key challenges, and lots crucial issues that it is of great importance to handle with it in order to truly realize the full potential of this technique and to paving the road to a robust transmission operation with raised performances in future communication systems.

In strict sense 'Mode division multiplexing', means that the modes (channels) are separate and should remain uncoupled and not interfere with each other (i.e. orthogonal). Hence, mode coupling (e.g. channels crosstalk) is the major obstacle for OAM-MDM. Channels crosstalk is obviated by either fiber design or multiple input multiple output digital signal processing (MIMO DSP) [9–11].

By carefully manipulating the fiber design parameters, it is possible to supervise the interactions between propagated modes and even control which modal basis is

incorporated: LP-fibers where the separation between vector modes are inferior to  $1 \times 10^{-4}$ , or OAM-fibers where the intermodal separation exceeds  $1 \times 10^{-4}$ , since either LP or OAM modes are constructed from fiber eigenmodes themselves [9]. This better facilitates understanding each fiber parameter impact and smooth the way of transition from design stage to fabrication process. Adding to that, exploit MIMO DSP is considered as the extreme choice to decipher channels at the receiving stage since it is heavy and complex. Its complexity is came from its direct proportionality to the transmission distance and to the number of modes. This allow it to become impractical in real time and threats the scalability of MDM in next generation optical communication system. For OAM-MDM systems using optical fibers, the fiber design stage is considered as the most crucial part and there is still a lot of opportunities for improved designs. New fiber designs for OAM mode transmission over short/medium and longer distances or among higher number of modes or possess a high performance metrics have been proposed and examined.

With the different related key challenges, this chapter offers a review of the state-of-the-art of SDM advances especially on OAM-MDM over optical fibers. In the first section, we discuss the SDM approaches as a solution to the expected capacity limit. The different mode basis supported in optical fibers are presented and discussed as either cylindrical vector modes, LP modes or OAM modes. The second section acts as a survey on recent advances (over last ten years) in OAM-MDM over optical fibers. We review the research effort invested in harnessing OAM as a degree of freedom to carry data in optical fiber networks. We summarized the key obtained results in the main family of optical fibers (i.e. conventional fibers and OAM specialty fibers) using OAM modes.

## 2. SDM over optical fibers

Space division multiplexing (SDM) has attracted high interest. It has revealed multiple directions of exploration and development. SDM consists of exploiting space-independent communication channels in both guided waves (e.g. optical fibers) or free space optical link (FSO). The channels' type vary depending in which factor of SDM we are exploiting; diversified cores, multiplexed LP modes or modes carrying OAM, multiple cores each supporting few multiplexed LP modes and so on.

Two main subset in SDM could be explored: core division multiplexing (CDM) where information is transmitted through cores (or fibers) of multicore fibers or mode division multiplexing (MDM), where information is transmitted through propagating modes of few or multimode fibers.

### 2.1 Core division multiplexing (CDM)

In principle, two main schemes are used. The first is based on the use of Single-core Fiber bundle (i.e. fiber ribbon) where parallels single mode fibers are packed together creating a fiber bundle or ribbon cable. The overall diameter of these bundles varies from around 10 mm to 27 mm. Fiber bundles deliver up to hundreds of parallel links. Fiber bundles have been commercially available [12, 13] and deployed in current optical infrastructure for several years already. Fiber bundles are also commercially used in conjunction with several SDM transceiver technologies [14].

The second scheme is based on carrying data on single cores (each core supports single mode) embedded in the same fiber known as Multicore Fibers (MCFs). Hence, each core is considered as an independent single channel (**Figure 1**).



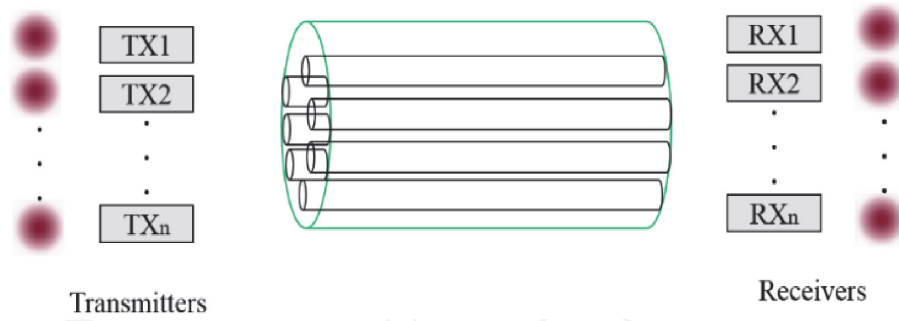


**Figure 1.**  
SDM through MCF.

The most important constraint in MCFs is the inter-core crosstalk (XT) caused by signal power leakage from core to its adjacent cores that is controlled by core pitch (distance between adjacent cores denoted usually as  $\Delta$ ) [15]. There are in Principle, two main categories of MCF: weakly coupled MCFs (=uncoupled MCF) and strongly coupled MCFs (=coupled MCF) depending on the value of a coupling coefficient 'K' (used to characterize the intercore crosstalk) [16–18]. Using the so-called supermodes to carry data, the crosstalk in coupled MCF must be mitigated by complex digital signal processing algorithms, such as multiple-input multiple-output digital signal processing (MIMO-DSP) techniques [19]. On the contrary, due to low XT in uncoupled MCF, it is not necessary to mitigate the XT impacts via complex MIMO. In principle, three crosstalk suppression schemes in uncoupled MCF could be incorporated, which are trench-assisted structure, heterogeneous core arrangement, and propagation-direction interleaving (PDI) technique [7].

The first paper on communication using MCF demonstrate a transmission of 112-Tb/s over 76.8 km in a 7-cores fiber using SDM and dense WDM in the C + L ITU-T bands. The spectral efficiency was of 14 b/s/Hz [20]. The second paper [21] shows an ultra-low crosstalk level ( $\leq -55$  dB over 17.6 km), which presents the lowest crosstalk between neighboring cores value to date. Other reported works, show high capacity (1.01Pb/s) [22] over 52 km single span of 12- core MCF. In [23], over 7326 km, a record of 140.7 Tb/s capacity are reached.

## 2.2 Mode division multiplexing (MDM)

Carrying data on optical fiber modes known as mode division multiplexing. In that scenario, each propagating mode is considered as independent channel [5, 24]. Two types of fiber are dedicated to support that strategy. One is based on the use of multimode fibers (MMF) while the second exploits the known few-mode fibers (FMF). The main difference between both is the number of modes (available channels). Since MMF can support large number of modes (tens), the intermodal crosstalk becomes large as well as the differential mode group delay (DMGD), where each mode has its own velocity, reducing the number of propagating modes along the fiber becomes viable solution. This supports FMF as a viable candidate for realizing SDM [5]. The concept of mode division multiplexing over a few/multi-mode fiber is illustrated in **Figure 2**.

Other kinds of optical fiber that can be used in MDM such as photonic crystal fibers (PCFs). Based on the properties of photonic crystals, PCF confines light by band gap effects, using air holes in their cross-sections, or by a conventional higher-index core modified by the presence of air holes. The PCF is built of one material (SiO<sub>2</sub>, As<sub>2</sub>S<sub>3</sub>, Polymers, etc), and air holes are introduced in the area surrounding the core providing the change of the refractive index contrast between the core and

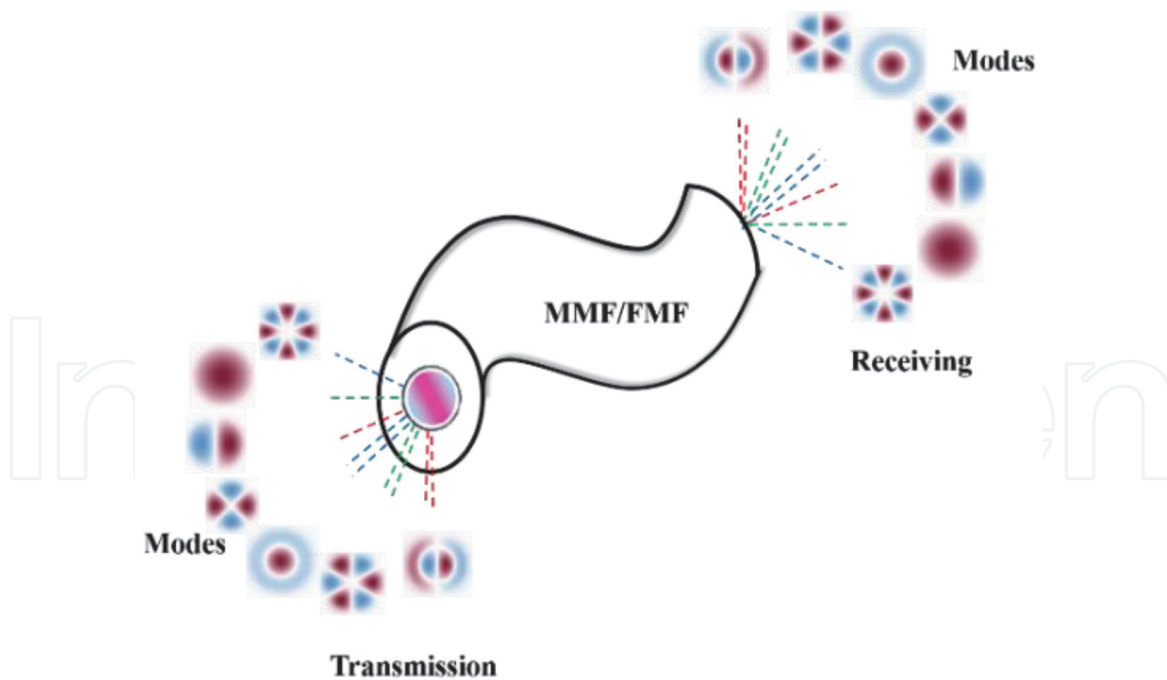


**Figure 2.**  
*The concept of mode division multiplexing over a FMF/MMF.*

the cladding. The transposition of air holes laid to form a hexagonal or circular lattice. **Figure 3** recapitalizes the principle SDM approaches over optical fibers [25].

2.3 Guided modes of optical fibers

We look into the different modal basis that can be supported by optical fibers. Like all electromagnetic phenomena, the propagation of optical fields along optical fiber is governed by Maxwell’s equations. Several modal basis can describe the

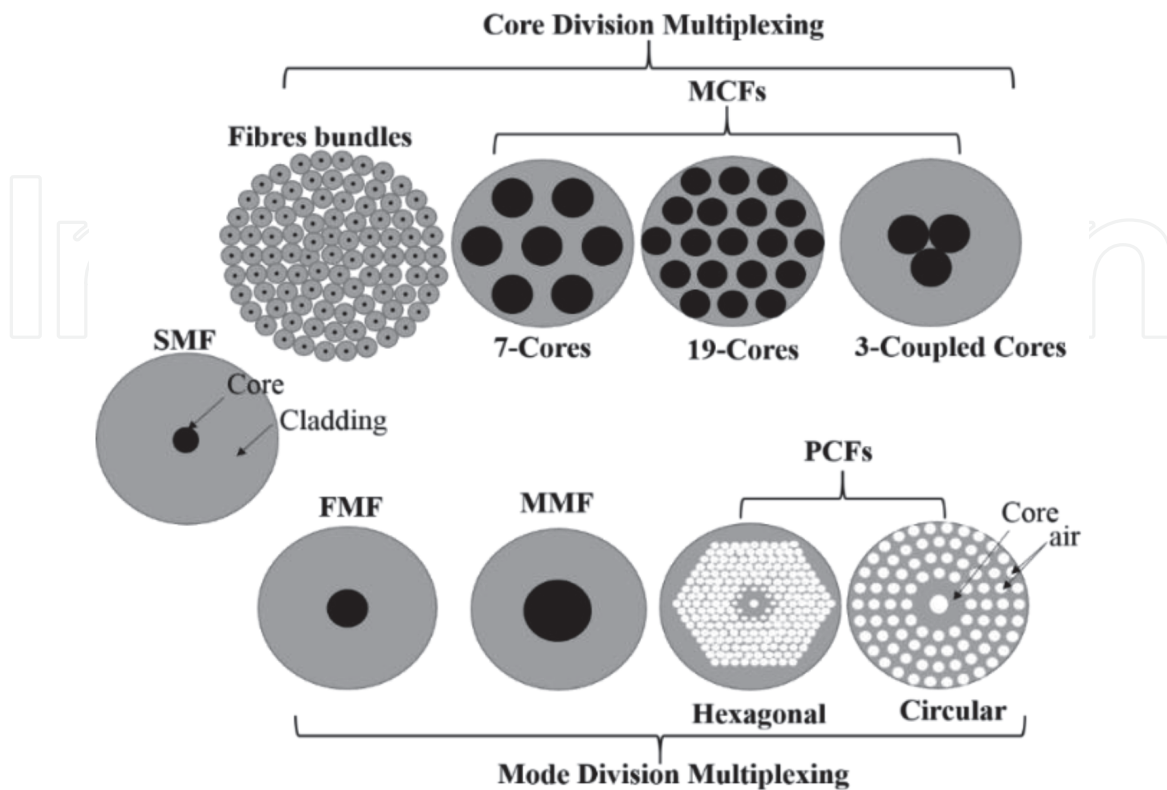


**Figure 3.**  
*Different approaches for SDM over optical fibers.*

propagation in optical fibers. In this chapter, fiber guided modes that we will meet are vector modes (i.e. fiber eigenmodes), linear polarized modes (i.e. LP modes) and orbital angular momentum modes (i.e. OAM modes). In the following, we provide general notions including mathematical expressions of modes of each mode basis.

### 2.3.1 Cylindrical vector modes

In the absence of the current in the medium, Maxwell equations are reduced to two homogeneous vector wave equations given by the following expressions [26]:

$$\left(\vec{\nabla}^2 + k^2 n^2\right) \vec{E} = -\vec{\nabla}(\vec{E} \cdot \vec{\nabla} \ln n^2) \quad (1)$$

$$\left(\vec{\nabla}^2 + k^2 n^2\right) \vec{H} = (\vec{\nabla} \times \vec{H}) \times \vec{\nabla} \ln n^2 \quad (2)$$

Where  $\vec{E}$  and  $\vec{H}$  are the electric and magnetic field respectively and  $n$  is the refractive index profile function. If we apply the boundary conditions according to the geometry and fiber refractive index, we get eigenvalues equation. Each solution of that equation is guided mode known by effective index  $n_{eff}$ . In cylindrical coordinates, for example, the electrical and magnetic fields are expressed as:

$$\begin{cases} \vec{E} = [\vec{r} E_r + \vec{\phi} E_\phi + \vec{z} E_z] \exp(j\beta z - j\omega t) \\ \vec{H} = [\vec{r} H_r + \vec{\phi} H_\phi + \vec{z} H_z] \exp(j\beta z - j\omega t) \end{cases} \quad (3)$$

Where  $E_r$ ,  $H_r$  are radial components,  $E_\phi$  and  $H_\phi$  are azimuthal components.  $\vec{r}$ ,  $\vec{\phi}$  and  $\vec{z}$  are unitary vectors.  $\beta = 2\pi n_{eff}/\lambda$  is the propagation constant of guided mode,  $\omega = 2\pi c/\lambda = kc$  is the pulsation;  $\lambda$  and  $c$  are the wavelength and light velocity both in vacuum, respectively. Guided modes in circularly symmetrical optical fiber are denoted as transverse electric ( $TE_{0,m}$ ) or transverse magnetic modes ( $TM_{0,m}$ ), if  $E_z = 0$  or  $H_z = 0$  respectively. Other kind of modes are  $HE_{\nu,m}$  and  $EH_{\nu,m}$  those where  $E_z \neq 0$  or  $H_z \neq 0$  (transverse components) are noted as hybrid modes. The designation  $HE_{\nu,m}$  stands for a hybrid mode for which  $H_z$  is dominant compared to  $E_z$ , while for  $EH_{\nu,m}$ ,  $E_z$  is dominant compared to  $H_z$ . The indexes  $\nu$  and  $m$  are the azimuthal and radial indices.  $\nu$  is related to the number of symmetry axes in the azimuthal dependency of the fields, and  $m$  is related to the number of zeros in the radial dependency of the fields.

Because of the circular symmetry, the field must keep the same value after a full  $2\pi$  azimuthal rotation, thus, the components  $E_z$  and  $H_z$  have a dependency according to  $\cos(\nu\phi)$  or  $\sin(\nu\phi)$ . hence, in circularly symmetrical optical fiber, hybrid modes are composed by two modes: one *even* while the other is *odd*. In the even mode, the radials components ( $E_r$ ) and azimuthal component ( $H_\phi$ ) are with  $\cos(\nu\phi)$  (i.e. Ox symmetry). The components  $E_\phi$  and  $H_r$  have dependency according to  $\sin(\nu\phi)$  (i.e. Oy symmetry). The radial, azimuthal and longitudinal electrical field components of even and odd modes are given by the following expressions:

$$\begin{cases} E_r^{even} = e_r(r) \cos(\nu\phi) \\ E_\phi^{even} = -e_\phi(r) \sin(\nu\phi) \\ E_z^{even} = e_z(r) \cos(\nu\phi) \end{cases} \quad (4)$$

$$\begin{cases} E_r^{\text{odd}} = e_r(r) \sin(\nu\phi) \\ E_\phi^{\text{odd}} = e_\phi(r) \cos(\nu\phi) \\ E_z^{\text{odd}} = e_z(r) \sin(\nu\phi) \end{cases} \quad (5)$$

The modes  $HE_{\nu,m}^{\text{even/odd}}$ ,  $HE_{\nu,m}^{\text{even/odd}}$ ,  $TE_{0,m}$  and  $TM_{0,m}$  are usually denoted as vector modes, cylindrical vector modes or fiber eigenmodes.

2.3.2 Scalar modes: LP modes

Frequently, the refractive index difference between core and cladding in optical fiber is very small ( $n_{\text{core}} \approx n_{\text{cladding}}$ ). We are then under the weakly guiding condition, and some approximations can be applied. The term “ $\nabla \ln n^2$ ” is neglected in expression 1. The wave equation becomes scalar. The resulted modes are linearly polarized designated usually as LP<sub>lm</sub> modes. LP modes are quasi-TEM guided modes, and have negligible  $E_z$  and  $H_z$  components. Therefore, they only have one component in the E field and one component in the H field (by convention, either  $E_x$  and  $H_y$ , or  $E_y$  and  $H_x$  in cartesian coordinates). This is why we call them scalar modes. The even modes are with  $\cos(l\phi)$ , while odd modes are varies with  $\sin(l\phi)$ .  $l$  is the azimuthal number while  $m$  has the same definition as in vector modes [26]. The electric field components of even and odd modes (after variable separation: radial and azimuthal) are given by the next expressions:

$$E_x^{\text{even}} = e_x(r) \cos(l\phi) \quad (6)$$

$$E_y^{\text{even}} = e_y(r) \cos(l\phi) \quad (7)$$

$$E_x^{\text{odd}} = e_x(r) \sin(l\phi) \quad (8)$$

$$E_y^{\text{odd}} = e_y(r) \sin(l\phi) \quad (9)$$

Practically, the LP modes come from linear combination between cylindrical vector modes. The correspondence between the linearly polarized modes and the conventional cylindrical vector modes is shown below (Table 1).

2.3.3 OAM modes

Optical fiber can support OAM modes by correctly superposing the even and odd modes for each  $HE_{l,m}$  and  $EH_{l,m}$  vector mode with  $\pm (\pi/2)$  phase shift [27, 28]. Taking into consideration the circular polarization of OAM states (spin); OAM modes are denoted as  $OAM_{\pm l,m}^\pm$  where  $\pm$  superscript describes the spin angular momentum (circular polarization),  $l$  and  $m$  subscript denote the azimuthal and

| Cylindrical vector modes          | LP modes                 | Cylindrical vector modes                                | LP modes                 |
|-----------------------------------|--------------------------|---|--------------------------|
| $HE_{1m}^{\text{odd}}$            | $LP_{0m}^y$              | $HE_{2m}^{\text{even}} - TM_{0m}$                       | $LP_{0m}^{\text{eveny}}$ |
| $HE_{1m}^{\text{even}}$           | $LP_{0m}^x$              | $HE_{(l+1)m}^{\text{odd}} + EH_{(l-1)m}^{\text{odd}}$   | $LP_{lm}^{\text{oddx}}$  |
| $HE_{2m}^{\text{odd}} + TE_{0m}$  | $LP_{1m}^{\text{oddx}}$  | $HE_{(l+1)m}^{\text{odd}} - EH_{(l-1)m}^{\text{odd}}$   | $LP_{lm}^{\text{oddy}}$  |
| $HE_{2m}^{\text{odd}} - TE_{0m}$  | $LP_{1m}^{\text{oddy}}$  | $HE_{(l+1)m}^{\text{even}} + EH_{(l-1)m}^{\text{even}}$ | $LP_{lm}^{\text{evenx}}$ |
| $HE_{2m}^{\text{even}} + TM_{0m}$ | $LP_{0m}^{\text{evenx}}$ | $HE_{(l+1)m}^{\text{even}} - EH_{(l-1)m}^{\text{even}}$ | $LP_{lm}^{\text{eveny}}$ |

Table 1.  
The correspondence between LP modes and the CV modes.



radial indices respectively.  $l$  is the topological number (number of twist in intensity profile),  $m$  describes the number of nulls radially (rings) in the intensity profile of the OAM mode. The magnitude of SAM equal  $\pm s\hbar$  where  $s = +1$  (left) or  $s = -1$  (right). The magnitude of OAM equals  $\pm l\hbar$ . The total angular momentum AM is the sum of SAM and OAM with a magnitude of  $(\pm l \pm s) \hbar$ .

For the  $TM_{0,m}$  and  $TE_{0,m}$  modes, the combination between them with a  $\pm (\pi/2)$  phase shift, carries the same magnitude of SAM and OAM but with opposite sign, making the total angular momentum equal to zero. This mode is not stable and cannot propagate, because the propagation constants of  $TE_{0,m}$  and  $TM_{0,m}$  modes are different. Therefore, we call this an unstable vortex. OAM modes made from  $HE_{l,m}$  modes would have a spin, but no topological charge ( $l = 0$ ). Therefore, this is not a true OAM mode, but simply a vector mode with circular polarization. However, we will consider it as  $OAM_{0,m}$ , in a more general definition.

OAM modes made from  $HE_{l,m}$  modes are rotating in the same direction as the spin (aligned spin-orbit modes), and OAM modes made from  $EH_{l,m}$  modes are rotating in the opposite direction as the spin (anti-aligned spin-orbit modes). If we take an even and an odd mode, with a  $\pi/2$  phase difference, and we sum the fields (expressions 1.5 and 1.6), we can get as a resulting field:

$$\begin{cases} E_r = e_r(r) \exp(\pm j\nu\phi) \\ E_\phi = je_\phi(r) \exp(\pm j\nu\phi) \\ E_z = e_z(r) \exp(\pm j\nu\phi) \end{cases} \quad (10)$$

The synthetic formula are as given in the following expressions

$$\begin{cases} HE_{l+1,m}^{even} \pm i \times HE_{l+1,m}^{odd} = OAM_{\pm l,m}^{L/R} \\ EH_{l-1,m}^{even} \pm i \times EH_{l-1,m}^{odd} = OAM_{\pm l,m}^{R/L} \\ TM_{0m} \pm jTE_{0m} = OAM_{\pm 1m}^{\pm} \end{cases} \quad (11)$$

To summarize, for a given topological charge  $l$ , there are four possible OAM modes: two different spin rotation, and two different phase rotation. This is illustrated in **Figure 4**. The only exceptions are for  $OAM_{\pm 1,m}$ , where spin and topological charge always have the same sign, and for  $OAM_{0,m}$ , where there is no topological charge (only spin) [28].

Moreover, others OAM construction formulas are explored based on two spatially orthogonal linear polarized (LP) modes owning orthogonal polarization

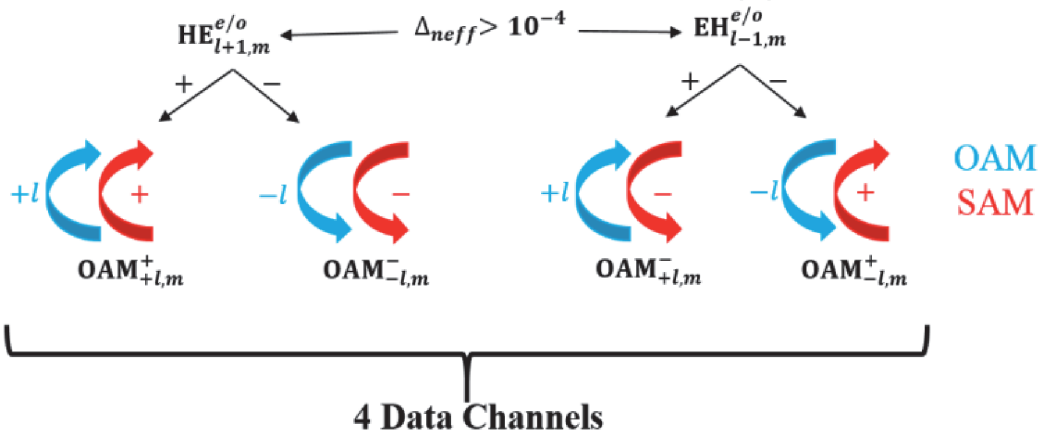


**Figure 4.**  
The four OAM mode degeneracies (reproduced from [28]).

directions (with a  $\pm \pi/2$  phase shift) which can be obtained by solving the scalar version of Maxwell equation (the scalar Helmholtz (wave) equation) under the weakly guiding approximation [29]. The LP-OAM synthetic formula are as follows:

$$\begin{Bmatrix} LP_{lm}^{ax} \pm iLP_{lm}^{bx} \\ LP_{lm}^{ay} \pm iLP_{lm}^{by} \end{Bmatrix} = F_{l,m}(r) \cdot \begin{Bmatrix} \vec{x}OAM_{\pm l,m} \\ \vec{y}OAM_{\pm l,m} \end{Bmatrix} \quad (12)$$

where  $\vec{x}$  and  $\vec{y}$  are the linear polarization along the x-axis and y-axis respectively,  $F_{l,m}(r)$  is the radial field distribution. The difference between OAM modes generated from fiber vector modes (CV-OAM) possess circular polarization while those generated from LP modes (LP-OAM) are the linear polarization (has no SAM).

### 3. OAM-MDM through optical fibers

OAM has seen application in optical communication due to the theoretically unprecedented quantities of data that can be modulated, multiplexed, transmitted and demultiplexed through either free space link (FSO as Free Space Optics), or optical fibers. Optical communications has exploited the physical dimension of optical signal to encode and transmit individual/separate/independent data stream through the same transmission medium (optical fiber or FSO). Since, the OAM is linked to the spatial phase distribution of light beam, it has been included under the space dimension as a subset or embodiment of SDM (space division multiplexing). In addition, since OAM is independent of wavelength, quadrature, and polarization, it provides an additional dimension for encoding information [30, 31]. The interest on OAM in communication (including optical, radio, underwater) has grown dramatically. **Figure 5(a)** and **(b)**, which highlights the number of published papers (conferences paper, books, journal papers and patents), translates that huge interest. In **Figure 5(a)**, we plot the number of published papers dealing with OAM in optical communication in last decade while **Figure 5(b)** shows the number of papers dealing with OAM in optical fibers, both are according to *Google Scholar*.

The worldwide backbone of high-capacity wired communications is optical fiber. The uses of OAM basis in optical fiber was a challenge to communication community. For a long time, optical fibers were only used for the generation or the transformation of OAM modes, and not for supporting their transmission [32]. The notion of transmitting OAM modes was demonstrated (theoretically, numerically,

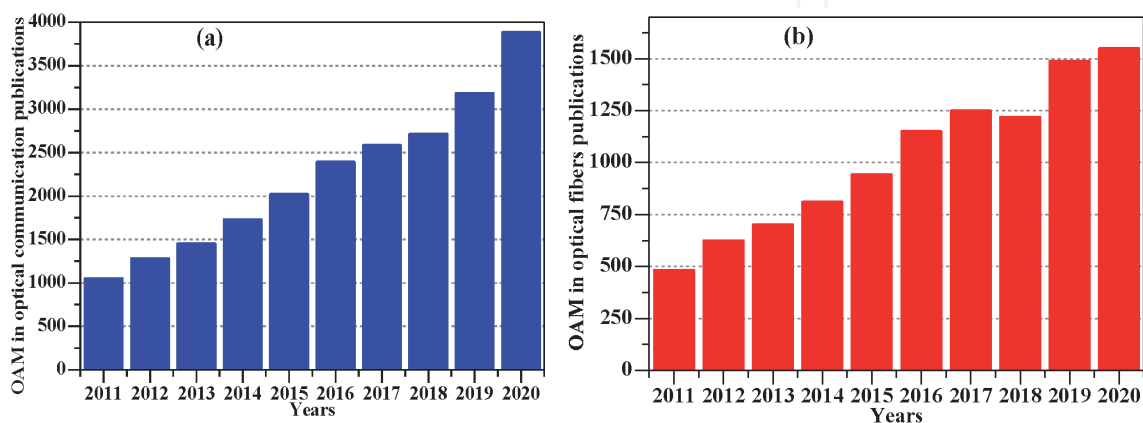


**Figure 5.** Number of papers published dealing with (a) OAM in optical communication over ten years (ranging from 2011 to 2020), (b) OAM in optical fibers over the same period (according to Google scholar).

and experimentally) through conventional optical fibers (classical deployed fibers), or specialty fibers that have been specifically designed to transmit robust OAM modes. In the following, we present kinds of optical fibers based on the consideration of their refractive indexes, (e.g. graded, step, ring, etc.), geometrical features (MMF, SMF, and FMF etc.) and transmission characteristics (MDM, CDM, PCF, kind of appropriate modes, etc.) and so on. We highlight the main design and principles results achievements.

### 3.1 Conventional fibers

Two examples of conventional optical fibers are multimode fiber MMF (e.g. OM1, OM2, OM3, OM4) where generally their refractive index are graded (GIF) and single mode fiber (e.g. G<sub>652</sub>) where the profile is step index (SMF). Conventional MMFs have large cores that are usually approximately 50  $\mu\text{m}$  and can support hundreds of modes. Due to severe inter-modal dispersion limitations, MMF were replaced by single mode fibers (SMFs) that have a relatively small core radius (not exceeding 10  $\mu\text{m}$ ). The refractive indexes of both fibers (OM3, and G<sub>652</sub> defined by ITU-T) are depicted in **Figure 6(a)** and **(b)**.

The most commonly used modal basis for fibers are LP modes. LP modes are not exact fiber modes, and can be simply viewed as combinations of fiber eigenmodes transverse (TE, TM, HE and EH) as indicated above.

Other type of fibers are few mode fibers (FMF) which consist of an improved version of MMF. They support a limited number of modes, as one of the key components for SDM for optical networks. The first paper that mentioned the possibility of transmitting OAM modes through optical fiber is from Alexeyev et al. in 1998 [33]. The authors demonstrated that the solution for OAM modes could exist in optical fibers (MMF). Considering the propagation of OAM modes through the cited fibers, the analysis of OAM in conventional graded index multimode fiber was reported (theoretically and numerically) [34]. In that paper, Chen and his co-authors presented a comprehensive analysis of the ten-OAM modes groups supported in OM3, including mode coupling, chromatic dispersion, differential group delay, effective mode area and nonlinearities.

Later on, the same team demonstrated experimentally the transmission of four-OAM mode group in OM3 MMF using mode exciting and filtering elements at the 2-fiber extremity. Moreover, they demonstrated two OAM mode groups transmission over 2.6-km MMF with low crosstalk free of MIMO-DSP [35]. In 2018, Wang et al. reported the successful transmission of OAM modes over 8.8-km OM4 MMF [36]. Wang and co-workers demonstrates a 120-Gbit/s quadrature phase-shift

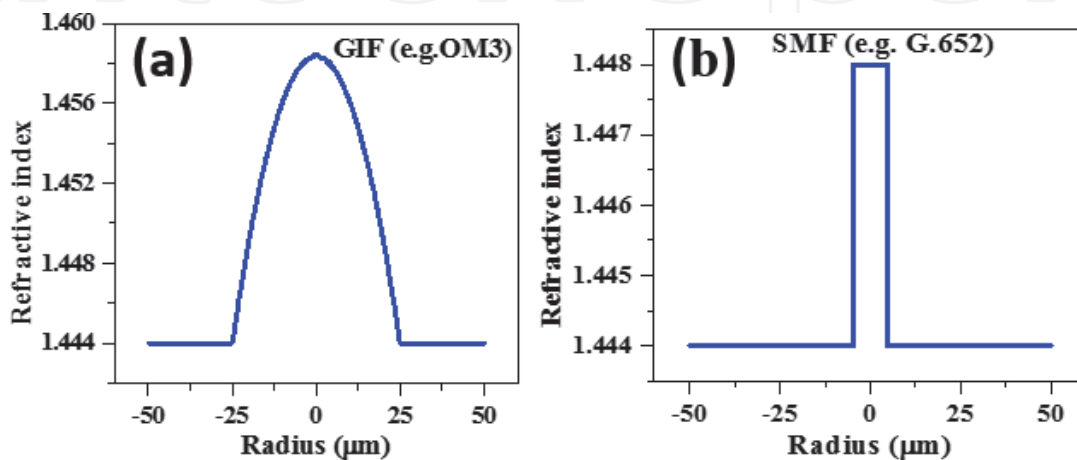


**Figure 6.** Refractive indexes of (a) graded index fiber (multimode fiber) and (b) step index fiber (single mode fiber).

keying (QPSK) signal transmission over 8.8-km OM 4 MMF with  $2 \times 2$  and  $4 \times 4$  MIMO-DSP. In second stage, they demonstrate the data-carrying two OAM mode groups (6 OAM states) multiplexing transmission over 8.8 km MMF without MIMO equalization.

The OAM in SMF (ITU-T G.652) was investigated, in [37]. The investigation was performed over 3 visible wavelengths (red at 632.8 nm, green at 532 nm, and blue at 476.5 nm) when G.652 becomes a few mode fiber. The synthesized OAM modes was investigated through effective mode area, nonlinearity, tolerance to fiber ellipticity and bending. The authors analyzed and estimated the fiber attenuation and bandwidth/capacity for OAM modes over six levels of wavelengths.

Few mode fibers (FMFs) with classical refractive index profile (step/graded), was used to transmit OAM modes. The transmission of OAM modes over FMF required a MIMO-DSP in combination with coherent detection to equalize the intermodal crosstalk. It was demonstrated in [38] the transmission of four OAM beams over 5-km FMF. Each transmitted OAM state carrying 20 Gbits/s QPSK data. MIMO DSP was used to mitigate the mode coupling effects. A graded index few mode fiber has been designed in [39] in order to support 10 OAM orders with high purity ( $\geq 99.9\%$ ) enabling low intermodal crosstalk ( $\leq -30$  dB). Later, in [40] Wang et al. demonstrated the viability of OAM modes transmission over both 50-km and 10-km FMFs. By adopting LDPC codes, the DMD and mode coupling was improved. In [41], Zhu et al. proposed and demonstrated a heterogeneous OAM based fiber by splicing 2 FMFs and MMF (OM3). Over 2 OAM modes, Zhu and co-workers transmit 20-Gbit/s QPSK data without MIMO-DSP. Recently, we proposed a family of graded index few mode fibers (four fibers) that supports 12 OAM states [42]. The evaluated differential group delay (DGD) and OAM purity demonstrate the viability of proposed fibers for short/medium haul connections.

### 3.2 OAM specialty fibers

OAM has changed the common features of optical fiber design guidelines. Cutting with the often-classical notion for imposing the center core to be the highest index of refractive (graded & step). In addition, the improvement of optical fibers fabrication technologies (materials & schemes) has made the fibers characterization no more challenging. New optical fibers with complicated shapes and high refractive index contrast have been experimentally characterized (demonstrated). The Modified Chemical Vapor Deposition (MCVD) is in principle one of the most fiber fabrication method that has been extensively used.

#### 3.2.1 OAM-fibers recommendations and design guidelines

Mainly three common features between OAM specialty fibers are identified. The first consists of the high contrast between core and cladding refractive indexes (jumps/contrasts) increasing the mode effective indices separation ( $\Delta n_{\text{eff}}$ ), hence enabling low induced crosstalk. The same feature involves the formation of OAM modes from cylindrical vector modes and avoid them to couple into LP modes. It is proved that minimum  $\Delta n_{\text{eff}}$  of  $10^{-4}$  is enough to keep robust OAM modes. This key value guarantees the minimum interaction between channels and prevents mode coupling inducing channels crosstalk XT. It has been demonstrated that through MCVD, a contrast of 0.14 is achievable with  $\text{GeO}_2$ - $\text{SiO}_2$  composition [43]. The second is about the refractive index profile that matches the donut shape of intensity profile of OAM mode (Ring shape: **Figure 7**). Thus, the Ring shaped (known also as depressed core fibers) has been extensively designed in OAM context instead of solid core fibers. Finally, the interfaces between fiber core and cladding preferred



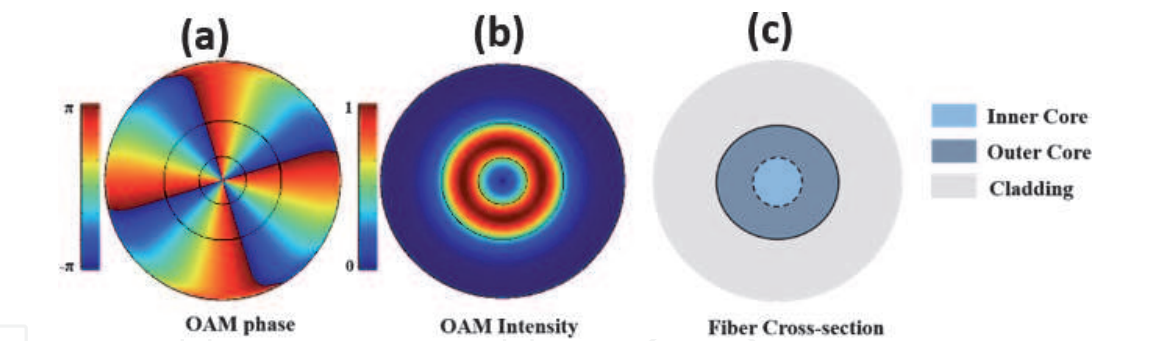


**Figure 7.** OAM mode (a) phases pattern (e.g.  $OAM_{4,1}$ ), (b) normalized intensity, (c) fiber cross-section with ring shape.

to be smoothed (instead of step (abrupt variation)) in order to eliminate the spin-orbit-coupling inducing OAM mode purity impairment and intrinsic crosstalk.

3.2.2 Vortex fibers (VFs)

The first specialty FMF designed for OAM modes is vortex fiber [44]. The designed fiber possess a good separation between co-propagating modes. Vortex fiber was first introduced to create cylindrical vector beams represented by  $TE_{0,1}$  and  $TM_{0,1}$  modes (also known as polarization vortices). Proposed by Ramachandran and al., Vortex fiber has a central core able to transmit the fundamental mode, surrounded by a lower trench, and an outer ring able to transmit the first OAM mode group. In first experience, they reported a transmission through more than 20 m fiber. Two years later, transmission of OAM through a 1 km fiber was reported [45–49]. **Figure 8** reported an optical microscope image of the end facet of the vortex fiber and the numerically calculated properties of the vortex fiber. All the experiments on OAM modes on the designed vortex fiber were summarized in [48].

3.2.3 Air Core fibers (ACFs)

Air core fiber (ACF) was proposed in [50]. 12 OAM modes were transmitted through 2 m of the fabricated ACF. Later on, 2 OAM modes were transmitted over 1 km of the fiber [51]. Among the main contributions, the authors demonstrated that OAM modes with higher  $l$  value are less sensitive to perturbations like bends and twists [52].

Within ROAM (revolution orbital angular momentum) project (EU H2020), Laval University (COPL) proposed and fabricated an ACF that achieved the record

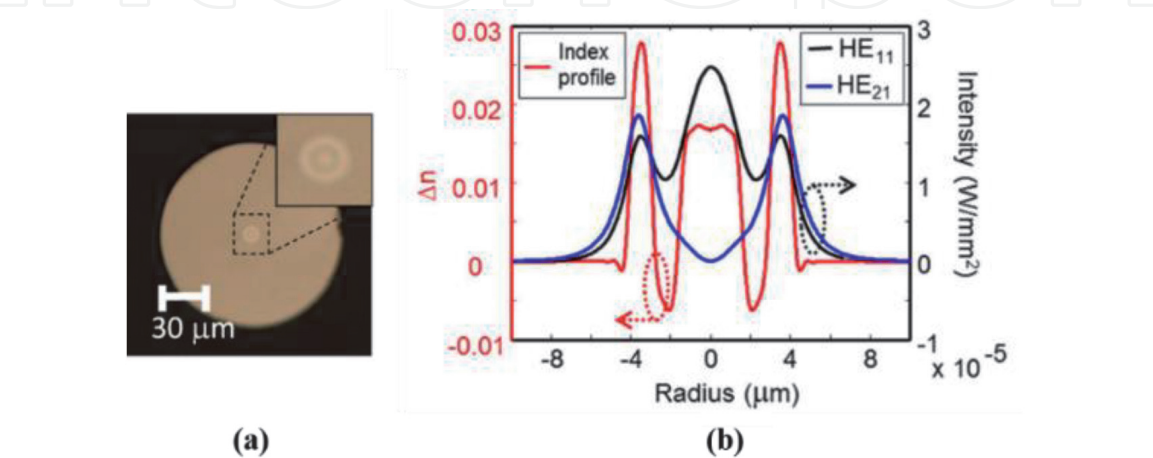


**Figure 8.** (a) Optical microscope image of vortex fiber, (b) numerically calculated properties [48].

of OAM modes transmitted through an optical fiber. Benefiting from the high refractive index contrast (air/silica), the fabricated fiber supports the transmission of 36 OAM states [53]. **Figure 9** shows the refractive index of ACF. Nevertheless, the designed fiber possess a very high loss (up to few dBs per meters) which make it unsuitable for communication. Recently, 10.56 Tbit/s has been demonstrated over 1.2 km ACF, without MIMO DSP, by carrying data over 12 OAM modes combined with wavelength division multiplexing (WDM) [54]. Latest air core ring fiber is designed to support more than 1000 OAM modes (using As<sub>2</sub>S<sub>3</sub> as ring material) across wide wavelength band covering S, O, E, S, C, and L Bands [55].

3.2.4 Inverse parabolic graded index fibers (IPGIFs)

Ung et al. proposed the inverse parabolic graded index FMF (IPGIF) to support OAM modes [56, 57]. The refractive index of IPGIF is given by the following expression:

$$n(r) = \begin{cases} n_2 \sqrt{(1 - 2N\Delta \left(\frac{r^2}{a^2}\right))} & 0 \leq r \leq a \quad (\text{core}) \\ n_3 & r \geq a \quad (\text{cladding}) \end{cases} \quad (13)$$

Where a, n<sub>1</sub>, n<sub>2</sub>, n<sub>3</sub> are the core radius, the refractive index at the core cladding interfaces, the refractive index at the core center and the refractive index of the cladding, respectively. The parameter N controls the shape of the IPGF. The refractive index of IPGF is presented in **Figure 10**. Based on a first-order perturbations, the authors highlighted the factors (refractive index, core radius and curvature shape) that directly related to enhance the intermodal separation in proposed IPGIF. Large refractive index gradient, high transverse field amplitude and large field variation are reasons of high intermodal separation enabling low crosstalk.

The designed IPG-FMF possess a good effective indices separation ( $\Delta n_{\text{eff}} > 2.1 \times 10^{-4}$ ) between its supported vector modes, and the transmission of eight OAM states (OAM<sub>±0,1</sub>, OAM<sub>±1,1</sub> and OAM<sub>±2,1</sub>) was demonstrated over 1 m which makes IPGIF suitable for short distances MDM transmission. On the other hand, the transmission of OAM<sub>±1,1</sub> over more than 1 km was demonstrated by experiment, which makes the novel fiber as a promising candidate for long-distance

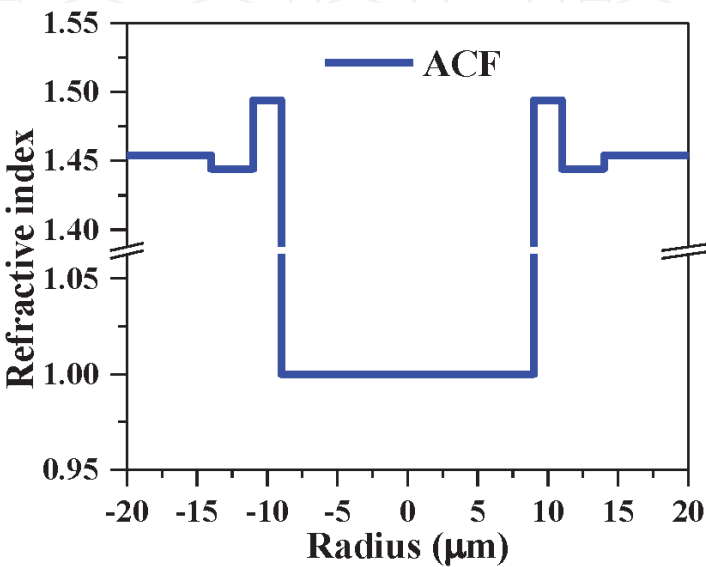


**Figure 9.**  
Refractive index profile of an air (hollow) core fiber (ACF).

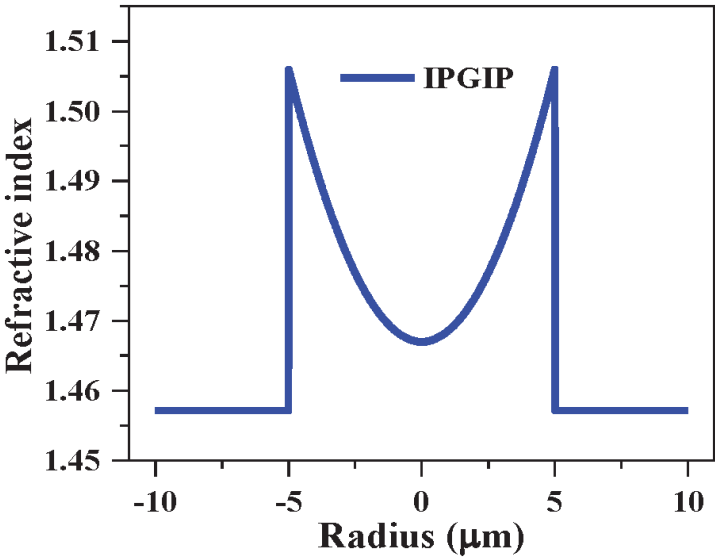


**Figure 10.**  
*Refractive index profile of inverse parabolic graded index fiber (IPGIF).*

OAM based MDM multiplexing system. Later on (2017), the multiplexing/ transmission and demultiplexing of 3.36 Tbits/s was demonstrated over 10-meters inverse parabolic graded index fiber by using four OAM modes and 15 wavelengths (WDM) [58].

3.2.5 Ring Core fibers (RCFs)

Due to the emerging interest in OAM-guiding fibers, already designed fiber for LP modes was investigated through OAM. The Ring core fiber (RCF), which has been introduced to minimize the differential group delay between LP modes, was tailored to support and transmit OAM modes. This interest on ring core fiber come from its refractive index profile that closely matches the annular intensity profile of OAM beams (**Figure 11**). C. Brunet et al. present an analytic tool to solve the vector version of Maxwell equations in RCF [59]. A fully vectorial description was reported in order to better tailor the RCF to OAM context. Using the modal map developed in [59], the group designed and manufactured a family of RCF (five fibers) suitable for OAM transmission [60]. In [61] S. Ramachandran et al. demonstrated the stability of OAM modes in RCF.

Recently, an RCF supported 50 OAM states divided into 13 mode groups (MGs) has been numerically investigated using small MIMO DSP blocks [62]. Experimentally, the transmission of two OAM mode-group is demonstrated over a 50 km ring core fiber without the use of MIMO DSP [63]. Emerging papers considering the

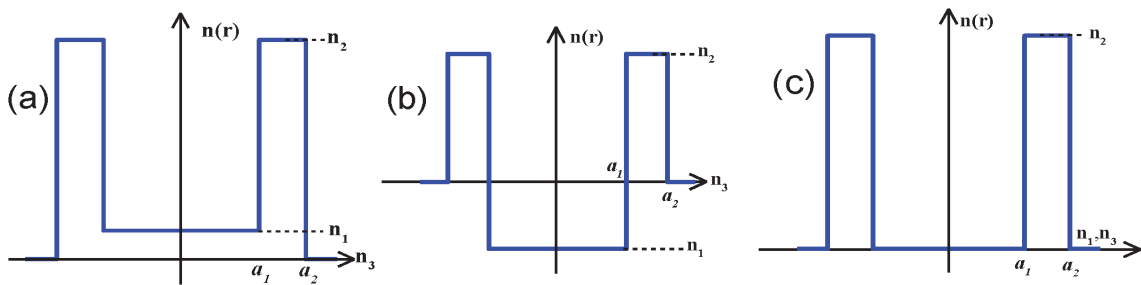


**Figure 11.**  
*Examples of RCF refractive index profiles: (a) RCF (higher center) (b) RCF (lower center) and (c) RCF,  $a_1$  and  $a_2$  are inner and outer core radius respectively.*

design of RCFs and the propagation demonstration of OAM modes through it that we should mention [64, 65].

3.2.6 Graded index ring Core fibers (GI-RCFs)

The ring notion touched the graded shape and a family of graded index ring core fibers (GI-RCF) has been proposed, designed and fabricated to support OAM mode group. **Figure 12** shows the refractive index of GI-RCF. In [66], Zhu and co-workers designed and fabricated the GI-RCF for OAM modes. The fiber supports 22 OAM modes with low insertion loss (less than 1 dB/km). The crosstalk between the highest order mode groups is less than 14 dB after 10-km propagation. With such fiber, a successful transmission of 32 Gbaud QPSk-data over 80 channels is experimentally demonstrated. A transmission capacity of 5.12 Tbits/s and a spectral efficiency of 9 bit/s/Hz, over 10 km propagation was reported [67].

The second demonstration was performed over 18-km propagation. Recently, the same group demonstrate the transmission of 12 Gbaud (8QAM) over 224 channels (2 OAM  $\times$  112 wavelengths). A transmission capacity of 8.4 Tbits/s was achieved without MIMO DSP because of the large high-order mode group separation of the OAM fiber [68].

To increase even further the capacity of the fiber link, OAM transmission was reported over uncoupled multi core fibers. While a complete review on this topic exceed the scope of this chapter, we can nevertheless mention some contributions. Li and Wang designed seven-ring core fiber (MOMRF) supporting 154 data-channels in total (22 modes  $\times$  7 rings) [69]. The proposed fiber featuring low-level inter-ring crosstalk ( $-30$  dB for a 100-km-long fiber) and intermodal crosstalk over a wide wavelength range (1520–1580 nm). Later, in [70], Li and Wang proposed a compact trench multi OAM ring fiber (TA-MOMRF) with 19 rings each supporting 22 modes (18 OAM states). The authors stated that such fiber is suitable for long distance OAM transmission enabling Pbit/s total transmission capacity and hundreds bit/s/Hz spectral efficiency. In [71], the authors proposed a coupled multi core fibers to support OAM modes (multi-orbital-angular-momentum (OAM)

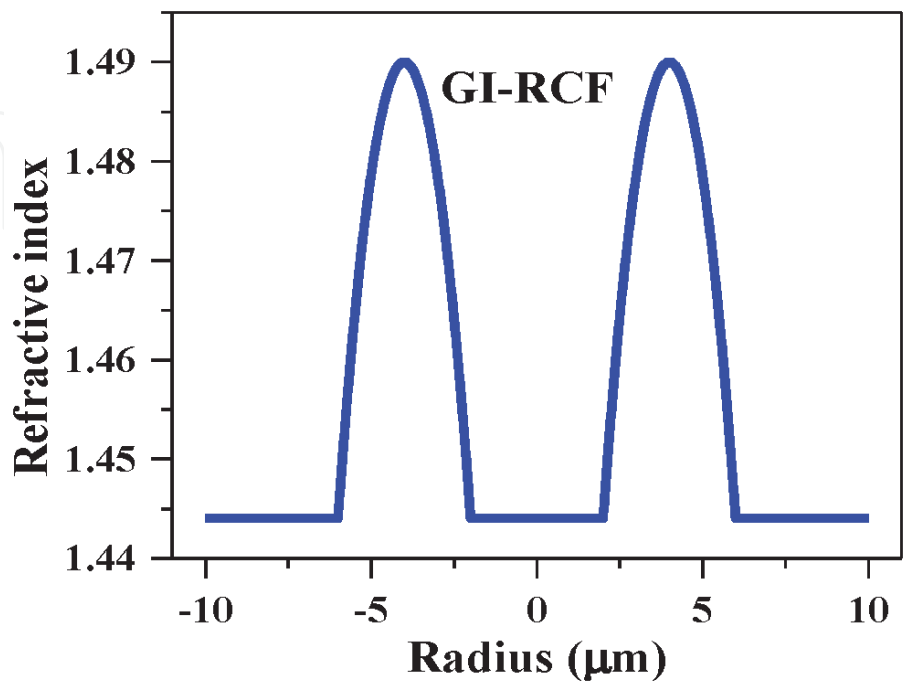


**Figure 12.**  
*Design of the GIRCF.*



multicore supermode fiber (MOMCSF). The designed supermode fiber show favorable performance of low mode coupling, low nonlinearity, and low modal dependent loss.

### 3.2.7 Inverse raised cosine few mode fibers (IRC-FMFs)

Using IPGI fiber as a benchmark, we proposed a novel fiber that is based on inverse raised cosine function (IRCF). The standard raised cosine function (RCF) when applied to a wideband signal steeply removes the high out-of-band signals, making the filtered signal highly purified. Moreover, RCF is used in the same context because it eliminates intersymbol interference [72]. The IRCF profile is given by the following expression [73]:

$$n(r) = \begin{cases} n_2 & \text{if } 0 \leq r \leq a \frac{1-\alpha}{2} \quad (\text{Core}) \\ -\frac{1}{2(n_2 - n_3)} \left( 1 + \cos \left[ \left( \frac{\pi}{a \times \alpha} \right) \left( r - a \frac{1-\alpha}{2} \right) \right] \right) & \text{if } a \frac{1-\alpha}{2} \leq r \leq a \frac{1+\alpha}{2} \quad (\text{Core}) \\ n_3 & \text{if } r \geq a \frac{1+\alpha}{2} \quad (\text{Cladding}) \end{cases} \quad (14)$$

where  $a$  is the core radius,  $n_1$  and  $n_2$  are respectively the maximum and the minimum refractive indices of the core,  $n_3$  is the refractive index of the cladding ( $r > a$ ), and  $\alpha$  is the profile shape. The refractive index of IRCF is shown in the **Figure 13**. The IRC profile is practically thinner (or more concentrated around the fiber axis) than the IPGI profile [73]. However, it is worthy to note that our profile becomes much smoother when reaching the maximum index value  $n_1$ . When compared with IPGI-FMF, the inverse-raised-cosine function offers a large modal separation. The enhanced separation is likely to hinder mode coupling, reducing the system crosstalk and improving the transmission. Moreover, IRC-FMF has the potential to handle OAM modes with high purity hence low intrinsic crosstalk [73, 74].

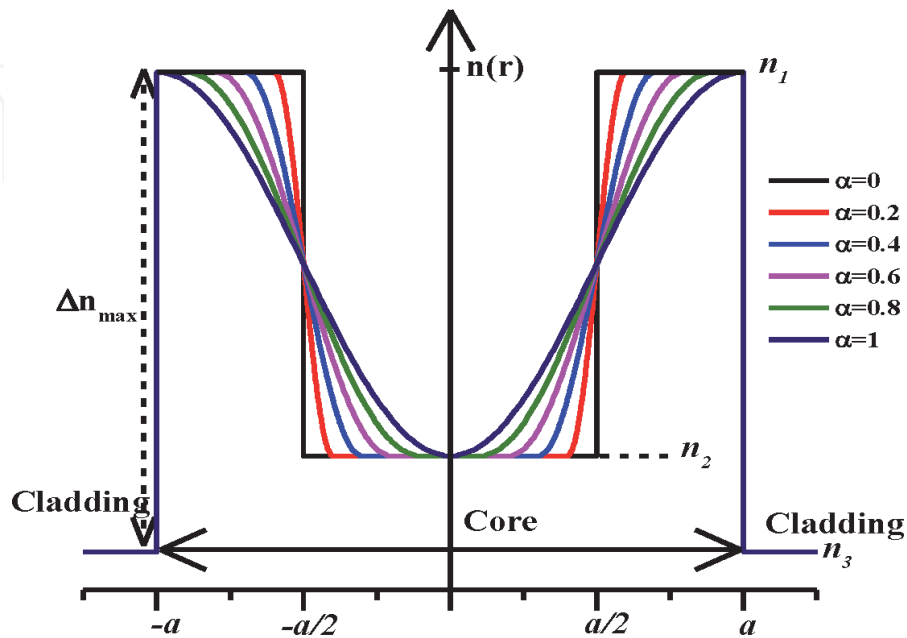


**Figure 13.** Index profiles of the IRC fiber (solid lines), with  $\alpha$  ranging from 0 to 1 (reproduced from 73).

3.2.8 Hyperbolic tangent few mode fibers (HTAN-FMFs)

Based on hyperbolic tangent function (HTAN), we proposed and designed a ring core few mode fiber that we refer to as hyperbolic tangent few mode fiber (HTAN-FMF). The function HTAN was not common in optical fiber profiling. It is widely used in various fields/domains such as digital neural networks, image processing, digital filters, and decoding algorithms [75–77] but not common in waveguide and optical fiber designs. Intuitively, one of the most attractive criteria in hyperbolic tangent function, used as an activation function in neural network, is its strong gradient centered around the inflection point (switch point). This is the same criteria required from an optical fiber profile in order to enhance the intermodal separation. The refractive index of HTAN-FMF is given by the following expression [78]:

$$n(r) = \begin{cases} n_2 \text{ if } 0 \leq |r| \leq a \frac{(1-\alpha)}{2} \text{ (Core)} \\ \frac{n_1+n_2}{2} + \frac{\Delta n}{2 \cdot \text{Tanh}(\pi)} \times \left[ \text{Tanh} \left( \frac{\pi \times (r-a_1)}{a_1 \times \alpha} \right) \right] \text{ if } a \frac{(1-\alpha)}{2} \leq |r| \leq a \frac{(1+\alpha)}{2} \text{ (Core)} \\ n_1 \text{ if } a \frac{(1+\alpha)}{2} \leq |r| \leq a \text{ (Core)} \\ n_3 \text{ if } |r| \geq a \text{ (Cladding)} \end{cases} \tag{15}$$

Where  $n_1, n_2, n_3$  are the refractive index at the core-cladding interface, at the core center, and at the cladding region, respectively.  $a, a_1$  and  $\alpha$  are the core radius, the half of core radius ( $a_1 = a/2$ ) and the shape parameter respectively.  $\Delta n$  is the actual refractive index difference (i.e.  $\Delta n = n_1 - n_2$ ) which corresponds to the extent of hyperbolic tangent function inside the core. The shape parameter  $\alpha$  controls the shape behavior of HTAN function. The refractive index of HTAN is illustrated in **Figure 14**. The proposed HTAN-FMF achieves a wide intermodal separation (between cylindrical vector modes) especially between  $TE_{0,1}$ ,  $HE_{2,1}$ , and  $TM_{0,1}$

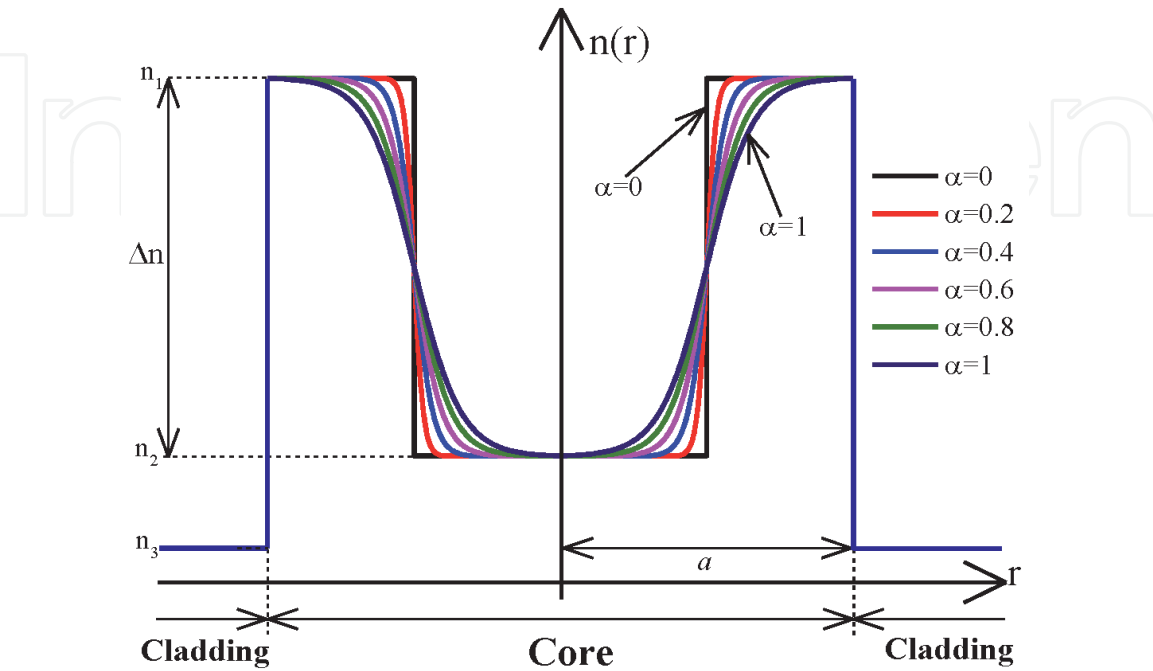


**Figure 14.**  
Refractive index profile of HTAN fiber for different values of profile shape  $\alpha$  [78].

( $\geq 3 \times 10^{-4}$ ). This enables low-level crosstalk channels carrying data during propagation and outperforms what is existing in the literature [78]. On the other hand, even with an exterior abrupt variation, the inner smooth behavior of HTAN-FMF guarantees the enhancement of the obtained OAM mode purities ( $\geq 99.9\%$ ) leading to intrinsic crosstalk as minimum as  $-30$  dB during propagation. Moreover, the obtained results in term of chromatic dispersion (max CD =  $-60$  ps/(km.nm)), differential group delay (max DGD =  $55$  ps/m), and bending insensitivity, demonstrate that the HTAN-FMF could be a viable candidate for enhancing the transmission capacity and the spectral efficiency in next generation OAM mode division Multiplexing (OAM-MDM) systems [78].

### 3.3 Photonic crystal fibers

Photonic crystal fibers (PCF) has shown its design flexibility to guide appropriate OAM modes. With adjustable parameters, PCF can offer more flexible design structures to provide unique fiber properties. Due to that, several kinds of OAM-PCF with various structures (hexagonal, circular, kagome...) and materials ( $\text{As}_2\text{S}_3$ ,  $\text{SiO}_2$ , polymer ...), having promising features have been designed and even fabricated. PCF have been proposed and fabricated to ensure good transmission quality of OAM modes. While a review on this topic exceed the scope of this thesis, we can nevertheless mention some details and contributions. PCFs supporting one, 2, 10, 12, 14, 26, 34, 42 and 48, first order OAM modes have been proposed featuring good transmission properties [79–89].

The race is still ongoing to increase the number of OAM modes in PCF featuring good transmission proprieties. To the best of our knowledge, the most supporting OAM modes number in a circular PCF reaches 110 over C + L communication bands [90]. The designed fiber featured large effective indices separation (are at the order of  $10^{-3}$ ), low nonlinear coefficient, low confinement loss (under  $10^{-7}$  dB/m), and relatively flat chromatic dispersion. Such fiber could find potential application in high capacity OAM-MDM system. By analysis of these recent mosaic OAM-PCFs literature, we can come to the general requirements in PCF design that ensure good transmission quality of OAM modes in the following five points or guidelines [91–94].

- Fiber index profile that matches the intensity profile of OAM modes (ring shape).
- The supported modes belonging to the same OAM mode family should possess a large index separation ( $\geq 10^{-4}$ ) to be free from complex and heavy multiple input multiple output digital signal processing (MIMO DSP) at the receiver side. This is achievable with high material contrast between the fiber core and the cladding. Instead of using pure  $\text{SiO}_2$  as a background material for the PCF-fiber, other available materials could be used such as Silicon (Si),  $\text{As}_2\text{S}_3$ , and Polymer.
- Large core thickness is required targeting to increase the supported OAM mode number.
- The excited OAM modes should be of the first order. Hence, it is preferable to avoid exciting the higher radial orders modes because it causes trouble in multiplexing and demultiplexing operations due to the intensity and phase variety distribution.

- The guided OAM modes would possess good transmission features such as low confinement loss, flat dispersion, large effective mode area, and low nonlinear coefficient over a large wavelength range (at least covering C + L bands defined by ITU-T).

#### 4. Conclusion

In this chapter, we have attempted to provide recent advances in SDM based Optical fibers. We showed that SDM is currently the unexhausted technology that can deal with the capacity need and boost data traffic. Furthermore, an interesting embodiment of SDM, which is based on carrying data on fiber modes (MDM) has been presented and discussed. The different mode basis supported in optical fibers are presented and discussed. Furthermore, we reviewed the research activities that are based on harnessing OAM modes to encode data channels either in classical optical fibers (i.e. with classical refractive index profiles) or in special fibers with appropriate ring profiles. We presented the main research activities and recent trends in OAM-MDM over the last ten years.

#### Author details


Alaaeddine Rjeb<sup>1\*</sup>, Habib Fathallah<sup>2</sup> and Mohsen Machhout<sup>1</sup>

<sup>1</sup> Laboratory of Electronic and Microelectronic, Faculty of Sciences of Monastir, Physics Department, University of Monastir, Monastir, Tunisia

<sup>2</sup> Laboratory of Artificial Intelligence and Data Engineering Applications, Faculty of Sciences of Bizerte, Computer Department, University of Carthage, Bizerte, Tunisia

\*Address all correspondence to: [alaaeddine.rjeb@gmail.com](mailto:alaaeddine.rjeb@gmail.com)

#### IntechOpen

© 2021 The Author(s). Licensee IntechOpen. This chapter is distributed under the terms of the Creative Commons Attribution License (<http://creativecommons.org/licenses/by/3.0>), which permits unrestricted use, distribution, and reproduction in any medium, provided the original work is properly cited. 



## References

- [1] Cisco VNI Global IP traffic forecast “2016–2021”.
- [2] A. Chrallyvy, Plenary paper: The coming capacity crunch. In: 2009 35th European Conference on Optical Communication, 2009, pp. 1–1.
- [3] Ellis, A. D., Mac Suibhne, N., Saad, D., & Payne, D. N. Communication networks beyond the capacity crunch. (2016).
- [4] R. Essiambre and R. Tkach. Capacity trends and limits of optical communication networks. In Proceedings of the IEEE, May 2012, vol. 100, no. 5, pp. 1035–1055.
- [5] Richardson, D. J., Fini, J. M., & Nelson, L. E. Space-division multiplexing in optical fibres. *Nature photonics*. 2013, 7(5), 354–362.
- [6] Saridis, G. M., Alexandropoulos, D., Zervas, G., & Simeonidou, D. Survey and evaluation of space division multiplexing: From technologies to optical networks. *IEEE Communications Surveys & Tutorials*. 2015; 17(4), 2136–2156.
- [7] Saitoh, K., & Matsuo, S. Multicore fiber technology. *Journal of Lightwave Technology*. 2016; 34(1), 55–66.
- [8] Yaman, F., Bai, N., Zhu, B., Wang, T., & Li, G. Long distance transmission in few-mode fibers. *Optics Express*. (2010); 18(12), 13250–13257.
- [9] L.A. Rusch, M. Rad, K. Allahverdyan, I. Fazal, E. Bernier, Carrying data on the orbital angular momentum of light, *IEEE Commun. Mag.* (2018), 56 (2) 219–224.
- [10] Bozinovic, N., Yue, Y., Ren, Y., Tur, M., Kristensen, P., Huang, H., & Ramachandran, S. Terabit-scale orbital angular momentum mode division multiplexing in fibers. *Science*. (2013), 340(6140), 1545–1548.
- [11] Wang, J., Yang, J. Y., Fazal, I. M., Ahmed, N., Yan, Y., Huang, H., & Willner, A. E. Terabit free-space data transmission employing orbital angular momentum multiplexing. *Nature photonics*, (2012), 6(7), 488–496.
- [12] “Sumitomo Electric.” [Online]. Available: <http://www.sumitomoelectric.com/>.
- [13] “OFS.” [Online]. Available: <http://www.ofsoptics.com>.
- [14] “Samtec.” [Online]. Available: <http://www.samtec.com>.
- [15] T. Hayashi, T. Taru, O. Shimakawa, T. Sasaki, and E. Sasaoka, “Design and fabrication of ultra-low crosstalk and low-loss multi-core fiber,” *Opt. Express*. 2011, vol. 19, no. 17, pp. 16576–16592.
- [16] Kingsta, R. M., & Selvakumari, R. S. A review on coupled and uncoupled multicore fibers for future ultra-high capacity optical communication. *Optik*. (2019), 199, 163341.
- [17] M. Koshiba, K. Saitoh, and Y. Kokubun, “Heterogeneous multi-core fibers: proposal and design principle,” *IEICE Electron. Express*. 2009, vol. 6, no. 2, pp. 98–103, Jan.
- [18] Y. Kokubun and M. Koshiba, “Novel multi-core fibers for mode division multiplexing: proposal and design principle,” *IEICE Electron. Express*. Apr. 2009, vol. 6, no. 8, pp. 522–528.
- [19] C. Xia, N. Bai, I. Ozdur, X. Zhou, and G. Li, “Supermodes for optical transmission,” *Opt. Express*. Aug. 2011, vol. 19, no. 17, pp. 16 653–16 664.
- [20] Zhu, B., Taunay, T. F., Fishteyn, M., Liu, X., Chandrasekhar, S., Yan, M. F., & Dimarcello, F. V. 112-Tb/s space-division multiplexed DWDM

- transmission with 14-b/s/Hz aggregate spectral efficiency over a 76.8-km seven-core fiber. *Optics Express*. (2011), 19(17), 16665–16671.
- [21] T. Hayashi, T. Taru, O. Shimakawa, T. Sasaki, and E. Sasaoka, Low-Crosstalk and Low-Loss Multi-Core Fiber Utilizing Fiber Bend. In: *Optical Fiber Communication Conference/National Fiber Optic Engineers Conference 2011, OSA Technical Digest (CD)* (Optical Society of America, 2011).
- [22] H. Takara, A. Sano, T. Kobayashi, H. Kubota, H. Kawakami, A. Matsuura, Y. Miyamoto, Y. Abe, H. Ono, K. Shikama, Y. Goto, K. Tsujikawa, Y. Sasaki, I. Ishida, K. Takenaga, S. Matsuo, K. Saitoh, M. Koshihara, and T. Morioka. 1.01-Pb/s (12 SDM/222 WDM/456 Gb/s) crosstalk-managed transmission with 91.4-b/s/Hz aggregate spectral efficiency. In: *the European Conf. Exhibition Optical Communication*, Amsterdam, the Netherlands, 2012.
- [23] K. Igarashi, et al., 1.03-Exabit/s·km Super-Nyquist-WDM Transmission over 7,326-km Seven-Core Fiber. *ECOC-2013*, PD1.E.3.
- [24] S. Berdague, and P. Facq, Mode Division Multiplexing in Optical Fibers. *App. Opt.* (1982), 24(11), 1950–1955.
- [25] Russell, P. Photonic crystal fibers. *Science*, (2003), 299(5605), 358–362.
- [26] J. Bures, *Guided Optics*, ser. Physics textbook. Wiley, 2009.
- [27] Zhang, H., Mao, B., Han, Y., Wang, Z., Yue, Y., & Liu, Y. Generation of orbital angular momentum modes using fiber systems. *Applied Sciences*, (2019), 9(5), 1033.
- [28] Brunet, C., & Rusch, L. A. Optical fibers for the transmission of orbital angular momentum modes. *Optical Fiber Technology*, (2017), 35, 2–7.
- [29] Ramachandran, S., & Kristensen, P. Optical vortices in fiber. *Nanophotonics*. (2013), 2(5–6), 455–474.
- [30] Yao, A. M., & Padgett, M. J. Orbital angular momentum: origins, behavior and applications. *Advances in Optics and Photonics*. (2011), 3(2), 161–204.
- [31] Padgett, M. J. Orbital angular momentum 25 years on. *Optics express*. (2017), 25(10), 11265–11274.
- [32] R. Kumar, D. S. Mehta, A. Sachdeva, A. Garg, P. Senthilkumaran, and C. Shakher. Generation and detection of optical vortices using all fiber-optic system. *Optics Communications*. 2008, vol. 281, no. 13, pp. 3414–3420.
- [33] A. N. Alexeyev, T. A. Fadeyeva, and A. V. Volyar, “Optical vortices and the flow of their angular momentum in a multimode fiber,” *Semiconductor Physics, Quantum Electronics & Optoelectronics*. 1998, vol. 1, no. 1, pp. 82–89.
- [34] Chen, S., & Wang, J. Theoretical analyses on orbital angular momentum modes in conventional graded-index multimode fibre. *Scientific Reports*. (2017), 7(1), 3990.
- [35] Zhu, L., Wang, A., Chen, S., Liu, J., Mo, Q., Du, C., & Wang, J. Orbital angular momentum mode groups multiplexing transmission over 2.6-km conventional multi-mode fiber. *Optics express*. (2017), 25(21), 25637–25645.
- [36] Wang, A., Zhu, L., Wang, L., Ai, J., Chen, S., & Wang, J. Directly using 8.8-km conventional multi-mode fiber for 6-mode orbital angular momentum multiplexing transmission. *Optics express*. (2018), 26(8), 10038–10047.
- [37] Chen, S., & Wang, J. Characterization of red/green/blue orbital angular momentum modes in conventional G. 652 fiber. *IEEE Journal*

- of Quantum Electronics. (2017), 53(4), 1–14.
- [38] G. Milione, H. Huang, M. Lavery, A. Willner, R. Alfano, T. A. Nguyen, and M. Padgett, “Orbital-angular-momentum mode (de)multiplexer: a single optical element for MIMO-based and non-MIMO-based multimode fiber systems. In: Optical Fiber Communication Conference, OSA Technical Digest (online) (Optical Society of America, 2014).
- [39] Zhang, Z., Gan, J., Heng, X., Wu, Y., Li, Q., Qian, Q., & Yang, Z. Optical fiber design with orbital angular momentum light purity higher than 99.9%. *Optics express*. (2015), 23(23), 29331–29341.
- [40] Wang, A., Zhu, L., Chen, S., Du, C., Mo, Q., & Wang, J. Characterization of LDPC-coded orbital angular momentum modes transmission and multiplexing over a 50-km fiber. *Optics express*, (2016), 24(11), 11716–11726.
- [41] Zhu, L., Wang, A., Chen, S., Liu, J., & Wang, J. Orbital angular momentum mode multiplexed transmission in heterogeneous few-mode and multi-mode fiber network. *Optics letters*. (2018), 43(8), 1894–1897.
- [42] Rjeb, A., Seleem, H., Fathallah, H., & Machhout, M. Design of 12 OAM-Graded index few mode fibers for next generation short haul interconnect transmission. *Optical Fiber Technology*. (2020), 55, 102148.
- [43] H. Doweidar. Considerations on the structure and physical properties of B2O3–SiO2 and GeO2–SiO2 glasses. *J. Non-Cryst. Solids*. (2011), 357(7), 1665–1670.
- [44] S. Ramachandran, P. Kristensen, and M. F. Yan, Generation and propagation of radially polarized beams in optical fibers. *Opt. Lett.* Aug. 2009, vol. 34, no. 16, pp. 2525–2527,.
- [45] N. Bozinovic, P. Kristensen, and S. Ramachandran, Long-range fiber-transmission of photons with orbital angular momentum. In: *CLEO: 2011 - Laser Applications to Photonic Applications*. Optical Society of America, 2011.
- [46] Bozinovic, N., Kristensen, P., & Ramachandran, S. Are orbital angular momentum (OAM/vortex) states of light long-lived in fibers. In: *Laser Science* (p. LWL3). Optical Society of America.
- [47] N. Bozinovic, S. Ramachandran, M. Brodsky, and P. Kristensen. Record-length transmission of entangled photons with orbital angular momentum (vortices). In: *Frontiers in Optics*, (2011, October). Optical Society of America, 2011.
- [48] N. Bozinovic, Y. Yue, Y. Ren, M. Tur, P. Kristensen, H. Huang, A. E. Willner, and S. Ramachandran, Terabit-scale orbital angular momentum mode division multiplexing in fibers. *Science*. 2013, vol. 340, no. 6140, pp. 1545–1548.
- [49] S. Golowich, P. Kristensen, N. Bozinovic, P. Gregg, and S. Ramachandran. Fibers supporting orbital angular momentum states for information capacity scaling. In: *Proc. of FIO*. OSA, 2012.
- [50] P. Gregg, P. Kristensen, S. Golowich, J. Olsen, P. Steinvurzel, and S. Ramachandran, “Stable transmission of 12 OAM states in air-core fiber: In *CLEO: 2013*. Optical Society of America, 2013.
- [51] P. Gregg, P. Kristensen, and S. Ramachandran. OAM stability in fiber due to angular momentum conservation. In *CLEO: 2014*. Optical Society of America, 2014.
- [52] Gregg, P., Kristensen, P., & Ramachandran, S. Conservation of orbital angular momentum in air-core optical fibers. *Optica*. (2015), 2(3), 267–270.



- [53] C. Brunet, P. Vaity, Y. Messaddeq, S. LaRoche, and L. A. Rusch, Design, fabrication and validation of an OAM fiber supporting 36 states. *Optics Express*. (2014), 22, no 21, pp. 26117–26127.
- [54] K. Ingerslev, P. Gregg, M. Galili, F. Da Ros, H. Hu, F. Bao, M. A. U. Castaneda, P. Kristensen, A. Rubano, L. Marrucci, and K. Rottwitt. 12 mode, WDM, MIMO-free orbital angular momentum transmission. *Opt. Exp.* Aug. 2018, vol. 26, pp. 20225–20232.
- [55] Y Wang, C. Bao, W. Geng, Y. Lu, Y. Fang, B. Mao, Y.-G. Liu, H. Huang, Y. Ren, and Z. Pan. Air-core ring fiber with >1000 radially fundamental OAM modes across O, E, S, C, and L bands. *IEEE Access*. 2020, vol. 8, pp. 68280–68287.
- [56] Ung, P. Vaity, L. Wang, Y. Messaddeq, L. A. Rusch and S. LaRoche. Few-mode fiber with inverse-parabolic graded-index profile for transmission of OAM-carrying modes. *Optics Express*. (July 2014), 22, no. 15, pp. 18044–18055.
- [57] Ung, B., Wang, L., Brunet, C., Vaity, P., Jin, C., Rusch, L. A., & LaRoche. S. Inverse-parabolic graded-index profile for transmission of cylindrical vector modes in optical fibers. In: *Optical Fiber Communication Conference*, (2014, March), (pp. Tu3K-4). Optical Society of America.
- [58] J. Zhu, et al. 3.36-Tbit/s OAM and Wavelength Multiplexed Transmission over an Inverse-Parabolic Graded Index Fiber. In: *CLEO 2017*, San Jose, p. SW4I.3, May 2017.
- [59] C. Brunet, B. Ung, P.-A. Bélanger, Y. Messaddeq, S. LaRoche, and L. A. Rusch. Vector mode analysis of ring-core fibers: design tools for spatial division multiplexing. *Journal of Lightwave Technology*. (2014), 32.23, 4046–4057.
- [60] C. Brunet, B. Ung, L. Wang, Y. Messaddeq, S. LaRoche, and L. A. Rusch. Design of a family of ring-core fibres for OAM transmission studies. *Optics Express*. (2015), 23.8: 10553–10563.
- [61] Ramachandran, S., Gregg, P., Kristensen, P., & Golowich, S. E. On the scalability of ring fiber designs for OAM multiplexing. *Optics express*. (2015), 23 (3), 3721–3730.
- [62] S. Chen, S. Li, L. Fang, A. Wang, and J. Wang. OAM mode multiplexing in weakly guiding ring-core fiber with simplified MIMO-DSP. *Opt. Exp.* 2019, vol. 27, no. 26, pp. 38049–38060.
- [63] R. Zhang, H. Tan, J. Zhang, L. Shen, J. Liu, Y. Liu, L. Zhang, and S. Yu. A novel ring-core fiber supporting MIMO-free 50 km transmission over high-order OAM modes. In: *Proc. Opt. Fiber Commun. Conf. (OFC)*, 2019, pp. 1–3.
- [64] Zhang, J., Wen, Y., Tan, H., Liu, J., Shen, L., Wang, M., & Yu, S. 80-Channel WDM-MDM transmission over 50-km ring-core fiber using a compact OAM DEMUX and modular 4×4 MIMO equalization. In: *Optical Fiber Communication Conference* (pp. W3F-3). Optical Society of America, (2019, March).
- [65] Banawan, M., Wang, L., LaRoche, S., & Rusch, L. A. Quantifying the Coupling and Degeneracy of OAM Modes in High-Index-Contrast Ring Core Fiber. *Journal of Lightwave Technology*. (2020), 39(2), 600–611.
- [66] Zhu, G., Chen, Y., Du, C., Zhang, Y., Liu, J., & Yu, S. A graded index ring-core fiber supporting 22 OAM states. In: *Opto-Electronics and Communications Conference (OECC) and Photonics Global Conference (PGC)*, 2017 (pp. 1–3). IEEE.
- [67] G. Zhu, et al. Scalable mode division multiplexed transmission over a 10-km ring-core fiber using high-order orbital



- angular momentum modes. Optics Express. vol. 26, pp. 594–604.
- [68] Zhu, L., Zhu, G., Wang, A., Wang, L., Ai, J., Chen, S. ... & Wang, J. 18 km low-crosstalk OAM+WDM transmission with 224 individual channels enabled by a ring-core fiber with large high-order mode group separation. Optics letters. (2018), 43(8), 1890–1893.
- [69] Li, S., & Wang, J. Multi-orbital-angular-momentum multi-ring fiber for high-density space-division multiplexing. IEEE Photonics Journal. (2013), 5(5), 7101007–7101007.
- [70] Li, S., & Wang, J. A compact trench-assisted multi-orbital-angular-momentum multi-ring fiber for ultrahigh-density space-division multiplexing (19 rings× 22 modes). Scientific reports. (2014), 4, 3853.
- [71] S. Li and J. Wang. Supermode fiber for orbital angular momentum (OAM) transmission. Opt. Express. Jul. 2015, vol. 23, pp. 18736–18745.
- [72] Proakis, J. G., Salehi, M., Zhou, N., & Li, X. (1994). Communication systems engineering (Vol. 2). New Jersey: Prentice Hall.
- [73] Rjeb, A., Guerra, G., Issa, K., Fathallah, H., Chebaane, S., Machhout, M., & Galtarossa, A. Inverse-raised-cosine fibers for next-generation orbital angular momentum systems. Optics Communications. (2020), 458, 124736.
- [74] Rjeb, A., Fathallah, H., & Machhout, M. Orbital Angular Momentum Mode Coupling Analysis due to Ellipticity and Birefringence in Inverse-raised Cosine Fiber. In: 2020 17th International Multi-Conference on Systems, Signals & Devices (SSD) (pp. 929–932). IEEE, (2020, July).
- [75] Garg, G., Sharma, P. An Analysis of Contrast Enhancement using Activation Functions. International Journal of Hybrid Information Technology. (2014), 7(5), 2.
- [76] Johansen, H. K., Sørensen, K., “Fast hankel transforms”, Geophysical Prospecting, 27(4), 876–901, (1979).
- [77] Goyal, A., Kwon, H. M. Hyperbolic tangent function avoided for encoded pilot low density parity check decoding. In: The European Conference on Wireless Technology, (pp. 149–152). IEEE, (2005, October).
- [78] Rjeb, A., Fathallah, H., Khaled, I., Machhout, M., & Alshebeili, S. A. A Novel Hyperbolic Tangent Profile for Optical Fiber for Next Generation OAM-MDM Systems. IEEE Access. (2020), 8, 226737–226753.
- [79] Wong, G. K. L., Kang, M. S., Lee, H. W., Biancalana, F., Conti, C., Weiss, T., & Russell, P. S. J. Excitation of orbital angular momentum resonances in helically twisted photonic crystal fiber. Science. (2012), 337(6093), 446–449.
- [80] Yue, Y., Zhang, L., Yan, Y., Ahmed, N., Yang, J. Y., Huang, H., ... & Willner, A. E. (2012). Octave-spanning supercontinuum generation of vortices in an As<sub>2</sub>S<sub>3</sub> ring photonic crystal fiber. Optics letters, 37(11), 1889–1891.
- [81] Zhang, H.; Zhang, W.; Xi, L.; Tang, X.; Tian, W.; Zhang, X. In: Proceedings of the Asia Communications and Photonics Conference, 2015, Hong Kong, China, pp. 1–3, 19–23 (November 2015).
- [82] Zhang, H., Zhang, X., Li, H., Deng, Y., Zhang, X., Xi, L., ... & Zhang, W. A design strategy of the circular photonic crystal fiber supporting good quality orbital angular momentum mode transmission. Optics Communications. (2017), 397, 59–66.
- [83] Zhang, H., Zhang, W., Xi, L., Tang, X., Zhang, X., & Zhang, X. A new type circular photonic crystal fiber for orbital angular momentum mode transmission.

IEEE Photonics Technology Letters.  
 (2016), 28(13), 1426–1429.

[84] Hu, Z. A., Huang, Y. Q., Luo, A. P., Cui, H., Luo, Z. C., & Xu, W. C. Photonic crystal fiber for supporting 26 orbital angular momentum modes. *Optics express*. (2016), 24(15), 17285–17291.

[85] Tian, W., Zhang, H., Zhang, X., Xi, L., Zhang, W., & Tang, X. A circular photonic crystal fiber supporting 26 OAM modes. *Optical Fiber Technology*. (2016), 30, 184–189.

[86] Chen, C., Zhou, G., Zhou, G., Xu, M., Hou, Z., Xia, C., & Yuan, J. A multi-orbital-angular-momentum multi-ring micro-structured fiber with ultra-high-density and low-level crosstalk. *Optics Communications*. (2016), 368, 27–33.

[87] Xi, X. M., Wong, G. K. L., Frosz, M. H., Babic, F., Ahmed, G., Jiang, X., ... & Russell, P. S. J. Orbital-angular-momentum-preserving helical Bloch modes in twisted photonic crystal fiber. *Optica*. (2014), 1(3), 165–169.

[88] Zhang, H., Zhang, X., Li, H., Deng, Y., Zhang, X., Xi, L., ... & Zhang, W. A design strategy of the circular photonic crystal fiber supporting good quality orbital angular momentum mode transmission. *Optics Communications*. (2017), 397, 59–66.

[89] Rjeb, A., Habib Fathallah, Saleh Chebaane, Mohsen Machhout Design of Novel Circular Lattice Photonic Crystal Fiber suitable for transporting 48 OAM modes. Accepted for publication in *Optoelectronics Letters* (2021). [In Press].

[90] Zhang, L., Zhang, K., Peng, J., Deng, J., Yang, Y., & Ma, J. Circular photonic crystal fiber supporting 110 OAM modes. *Optics Communications*. (2018), 429, 189–193.

[91] Li, H., Ren, G., Zhu, B., Gao, Y., Yin, B., Wang, J., & Jian, S. Guiding

terahertz orbital angular momentum beams in multimode Kagome hollow-core fibers. *Optics letters*. (2017), 42(2), 179–182.

[92] Zhang, H., Zhang, X., Li, H., Deng, Y., Xi, L., Tang, X., & Zhang, W. The orbital angular momentum modes supporting fibers based on the photonic crystal fiber structure. *Crystals*. (2017), 7(10), 286.

[93] Zhang, H., Zhang, X., Li, H., Deng, Y., Zhang, X., Xi, L., & Zhang, W. A design strategy of the circular photonic crystal fiber supporting good quality orbital angular momentum mode transmission. *Optics Communications*. (2017), 397, 59–66.

[94] Li, H., Zhang, H., Zhang, X., Zhang, Z., Xi, L., Tang, X. ... & Zhang, X. Design tool for circular photonic crystal fibers supporting orbital angular momentum modes. *Applied optics*. (2018), 57(10), 2474–2481.